

Time domain analysis of optical amplification in Er³⁺ doped SiO₂-TiO₂ planar waveguide

D. Biallo¹, A. D'Orazio¹, M. De Sario¹, V. Petruzzelli¹, F. Prudeniano²

¹ Dipartimento di Elettrotecnica ed Elettronica, Politecnico di Bari, Via Orabona 4, 70124 Bari

² Dipartimento di Ingegneria dell'Ambiente e per lo Sviluppo Sostenibile, Politecnico di Bari,
Via del Turismo 8, 74100 Taranto
dorazio@poliba.it

Abstract: A time domain analysis of light amplification in an erbium doped silica-titania planar waveguide is reported. The investigation is performed by means of a home-made computer code which exploits the auxiliary differential equation scheme combined with the finite difference time domain technique to solve Maxwell's equations and the rate equations. The simulation model takes into account the pump and input signal propagation, the secondary transitions pertaining to the ion-ion interactions and exploits the optical, spectroscopic and geometrical parameters measured on the fabricated waveguide.

©2005 Optical Society of America

OCIS codes: (190.0190) Nonlinear Optics; (140.0140) Lasers and laser optics; (250.5980) Optoelectronics

References and Links

1. P.G.Kik, A.Polman, "Cooperative Upconversion as the Gain-Limiting Factor in Er Doped Miniature Al₂O₃ Optical Waveguide Amplifiers," J. Appl. Phys. **93**, 5008-5012 (2003).
2. M.Federighi, I.Massarek, P.F.Trwoga, "Optical Amplification in Thin Optical Waveguides with High Er Concentration," IEEE Photon. Technol. Lett. **5**, 227-229 (1993).
3. F.Di Pasquale, M.Federighi, "Modelling of Uniform and Pair-Induced Upconversion Mechanism in High-Concentration Erbium-Doped Silica Waveguides," J. Lightwave Technol. **13**, 1858-1864 (1995).
4. W.J.Miniscalco, R.S.Quimby, "General Procedure for Analysis of Er³⁺ Cross Section," Opt. Lett. **16**, 258-260 (1991).
5. A.D'Orazio, M.De Sario, L.Mescia, V.Petruzzelli, F.Prudeniano, A.Chiasera, M.Montagna, C.Tosello, M.Ferrari, "Design of Er³⁺ Doped SiO₂-TiO₂ Planar Waveguide Amplifier," J. Non-Crystalline Solids **322**, 278-283 (2003).
6. A.Taflove, S.C.Hagness, "Computational Electrodynamics: the Finite-Difference Time-Domain Method," (Artech House Boston-London, 2000)
7. A.D'Orazio, V.De Palo, M.De Sario, V.Petruzzelli, F.Prudeniano, "Finite Difference Time Domain Modeling of Light Amplification in Active Photonic Band Gap Structures," Progress in Electromagnetics Research PIER **39**, 299-339 (2003).
8. A.S.Nagra, R.A.York, "FDTD Analysis of Wave Propagation in Nonlinear Absorbing and Gain Media," IEEE Trans. Antennas Prop. **46**, 334-340 (1998).
9. X. Jiang, C. M. Soukoulis, "Time Dependent Theory for Random Lasers," Phys. Rev. Lett. **85**, 70-73 (2000).
10. S.Chang, A. Taflove, "Finite-Difference Time Domain Model of Lasing Action in a Four-Level Two-Electron Atomic System," Opt. Express **12**, 3827-3833 (2004).
11. K. Jinguji, M. Horiguchi, S. Shibata, T. Kanamori, S. Mitachi, T. Manabe, "Material Dispersion in Fluoride Glasses," Electron. Lett. **18**, 164-165 (1982).
12. C. Tosello, F. Rossi, S. Ronchin, R. Rolli, G.C. Righini, F. Pozzi, S. Pelli, M. Fossi, E. Moser, M. Montagna, M. Ferrari, C. Duverger, A. Chiappini, C. De Bernardi, "Erbium-Activated Silica-Titania Planar Waveguides on Silica-on-Silicon Substrates Prepared by rf Sputtering," J. Non-Crystalline Solids **284**, 243-248 (2001).
13. A.E.Siegman, "Lasers" (University Science Book 1986)

1. Introduction

The Er³⁺ doped channel waveguide amplifiers (EDWA) have recently become very attractive in the field of the third window optical fiber communications. These devices show very

interesting potential applications, overall for the possibility of integration with pump lasers and optical devices.

To obtain high gain figures in a compact length, high values of the Er^{3+} concentration are necessary but in this way the concentration quenching effects become very considerable and detrimental to the optical gain, since they reduce the population in the first excited state [1-3]. Therefore, an accurate model of the optical amplification in an erbium doped structure must include both processes of a) the cross relaxation mechanism, in which an excited Er^{3+} ion excites a neighbouring unexcited Er^{3+} ion, and of b) cooperative upconversion, in which an excited Er^{3+} ion promotes a neighbouring excited Er^{3+} ion into a higher lying state.

To model optical gain various solutions were proposed in literature. A frequency domain method was implemented using the Runge-Kutta iterative method, that solves the rate equations, the equations of pump and signal powers propagation and the equation of spectral density of noise power due to the amplified spontaneous emission (ASE) along the propagation direction of the active media [4, 5].

Finite-difference time domain method has also been used to model gain in lasers by including a frequency-dependent negative conductivity term in Maxwell's equations [6,7]. This last formulation is based on the assumption that the gain and the absorption of the medium are independent on signal intensity and depend only on the frequency. This approach is reasonable for small signal intensities and for slowly varying pulses; when larger signal intensities or rapidly varying signals are considered, the analysis could be not correct, due to the change in atomic populations with time and to signal induced transitions. An auxiliary differential equation finite-difference time domain (ADE-FDTD) scheme has been proposed [8,9] in order to take into account the rate equations that give the energy states population time variation during the propagation of pump and input signals. The model was applied to an absorber comprising a two-level atomic system and to a gain medium consisting of a four-level atomic system. Recently a new finite-difference time domain computational model of the lasing dynamics of a four-level two electron atomic system has been described, where transitions between the energy levels are governed by coupled rate equations and the Pauli Exclusion Principle [10].

In this paper we propose a time domain analysis of the amplification phenomenon in an erbium doped waveguide, based on a reformulation of the ADE-FDTD technique which solves at the same time the Maxwell equations and the rate equations. To perform an exact analysis, the concentration quenching effects are taken into account. Although the time domain method requires high computational time, which increases by increasing the device dimensions, it allows to obtain the amplification factor in a frequency spectrum in a single run. The numerical investigation is performed by means of a home-made computer code which includes the relevant measured spectroscopic and optical parameters of the Er^{3+} doped $\text{SiO}_2\text{-TiO}_2$ planar waveguide fabricated by rf sputtering [11-12]. The choice of $\text{SiO}_2\text{-TiO}_2$ binary system as host material is due to the fact that it is possible to easily control the refractive index by changing the $\text{SiO}_2\text{-TiO}_2$ molar ratio: this fact allows to optimize the amplifier performance.

2.Theory

The analysis of optical amplification in the erbium doped $\text{SiO}_2\text{-TiO}_2$ waveguide is performed by solving simultaneously a) the erbium rate equations which model the time evolution of the atomic energy level populations, b) the Maxwell equations and c) the auxiliary differential equation, i.e. the electron oscillator (EO) equation that takes into account the field effect on the medium during its propagation.

The ion transitions among the energy levels of the EDWA are summarized in Fig. 1. By using a pump beam at the wavelength $\lambda_p = 980$ nm, the typical transitions of the four-level laser systems occur. In particular, the ions at the ground state level $I_{15/2}$ (level 1) are excited to the level $I_{11/2}$ (level 3), the ground state absorption (GSA) cross-section having a peak at this wavelength. The optical gain, via the laser transition, $I_{13/2} \rightarrow I_{15/2}$, occurs at the wavelength $\lambda_a = 1532$ nm, where the peak of stimulated emission (SE) takes place. The model, implemented in

the ADE-FDTD computer code, includes the following other phenomena: (a) the up-conversion, C_{up} , due to ion pairs excited in the signal level $I_{13/2}$ (level 2), which results in the population of the $I_{9/2}$ level (level 4); (b) the up-conversion, C_3 , due to two neighbour ions excited in the pump level $I_{11/2}$, which results in the population of the $F_{7/2}$ level; (c) the cross-relaxation, C_{14} , between an ion excited in the level $I_{9/2}$ and an ion in the ground state $I_{15/2}$ which, by energy transfer, leave both in the level $I_{13/2}$. The rate equations corresponding to the four-level system are the following:

$$\frac{dN_4}{dt} = -\frac{N_4}{\tau_{43}} + C_{up} \cdot N_2^2 + C_3 \cdot N_3^2 - C_{14} \cdot N_1 \cdot N_4 \quad (1)$$

$$\frac{dN_3}{dt} = W_p \cdot N_1 - \frac{N_3}{\tau_{32}} + \frac{N_4}{\tau_{43}} - 2 \cdot C_3 \cdot N_3^2 \quad (2)$$

$$\frac{dN_2}{dt} = \frac{N_3}{\tau_{32}} + \frac{\mathbf{e}(t) \cdot \mathbf{dp}(t)}{h\nu_s} - \frac{N_2}{\tau_{21}} + 2 \cdot C_{14} \cdot N_1 \cdot N_4 - 2 \cdot C_{up} \cdot N_2^2 \quad (3)$$

$$\frac{dN_1}{dt} = -W_p \cdot N_1 - \frac{\mathbf{e}(t) \cdot \mathbf{dp}(t)}{h\nu_s} + \frac{N_2}{\tau_{21}} - C_{14} \cdot N_1 \cdot N_4 + C_{up} \cdot N_2^2 + C_3 \cdot N_3^2 \quad (4)$$

where N_i are the population densities, the label i indicating the i -th level of the erbium ion, the concentration quenching coefficients C_{up} and C_3 take into account the up conversion while C_{14} is the cross relaxation coefficient, W_p is the pumping rate, $\mathbf{e}(t)$ is the electric field vector, $\mathbf{p}(t)$ is the electric polarization vector, τ_{ij} are the lifetimes between the i -th and j -th levels; the term $\frac{\mathbf{e}(t) \cdot \mathbf{dp}(t)}{h\nu_s} \cdot \frac{dp(t)}{dt}$ is the excitation rate.

The population densities N_i are linked by the conservation equation:

$$N_T = N_1 + N_2 + N_3 + N_4 \quad (5)$$

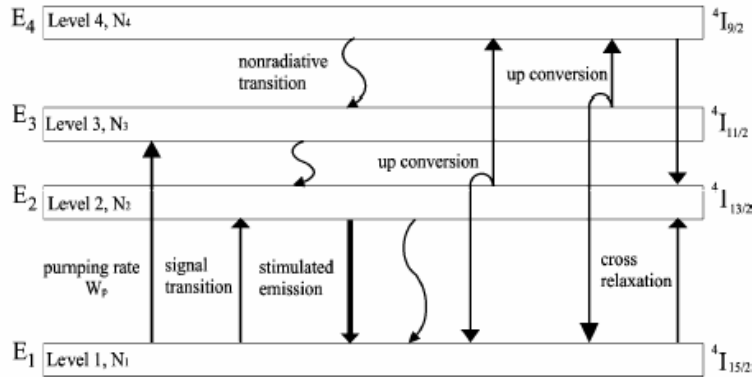


Fig. 1. Energetic level transitions of an erbium system

The time dependent Maxwell equations in Cartesian formulation:

$$\begin{aligned}\nabla \times \mathbf{h}(\mathbf{t}) &= \frac{\partial \mathbf{d}(\mathbf{t})}{\partial t} \\ \nabla \times \mathbf{e}(\mathbf{t}) &= -\mu_0 \frac{\partial \mathbf{h}(\mathbf{t})}{\partial t}\end{aligned}\quad (6)$$

are explicated in terms of the electric flux density \mathbf{d} , while \mathbf{h} is the magnetic field and μ_0 is the vacuum magnetic permeability.

The expression of the electric flux density $\mathbf{d}(\mathbf{t})$ in terms of the polarization $\mathbf{p}(\mathbf{t})$ allows to link the Maxwell equations to the auxiliary differential equation derived by the classic electron oscillator (CEO) model, opportunely modified in order to be applied to a collection of resonant atoms:

$$\mathbf{d}(\mathbf{t}) = \varepsilon_0 \mathbf{e}(\mathbf{t}) + \mathbf{p}_{\text{at}}(\mathbf{t}) + \mathbf{p}_{\text{host}}(\mathbf{t}) \quad (7)$$

being ε_0 the free space dielectric permeability. The polarization $\mathbf{p}(\mathbf{t})$ has been expressed as the sum of two terms, \mathbf{p}_{host} and \mathbf{p}_{at} , corresponding to the polarization due to the host dielectric material and the resonant polarization produced by the laser atoms, respectively [13].

The resonant electric polarization \mathbf{p}_{at} and the electric field for an isotropic medium are linked by the modified electron oscillator (MEO) equation:

$$\frac{d^2 \mathbf{p}_{\text{at}}(\mathbf{t})}{dt^2} + \Delta \omega_a \frac{d \mathbf{p}_{\text{at}}(\mathbf{t})}{dt} + \omega_a^2 \mathbf{p}_{\text{at}}(\mathbf{t}) = k \Delta N_{12}(\mathbf{t}) \mathbf{e}(\mathbf{t}) \quad (8)$$

where the resonance frequency ω_a is the characteristic transition frequency related to the energy levels involved in the stimulated emission, given by:

$$\omega_a = \frac{E_2 - E_1}{\hbar} \quad (9)$$

where \hbar is the reduced Planck constant and E_1 and E_2 are the energy levels involved in the transition.

To take into account the fact that in an actual atomic system there are almost always perturbation effects, or de-phasing effects, which randomize the time-phases of individual dipole oscillators and hence cause the macroscopic polarization $\mathbf{p}_{\text{at}}(\mathbf{t})$ to become much smaller than the value foreseen by the model of CEO, the total energy decay rate $\Delta \omega_a$, which is the full width at half maximum (FWHM) linewidth of the atomic transition, is expressed by:

$$\Delta \omega_a = \gamma_r + \gamma_{\text{nr}} + \frac{2}{T_2} \quad (10)$$

where γ_r and γ_{nr} are the energy radiative and non-radiative decay rates, respectively. T_2 is the mean time between de-phasing events.

Moreover, in the MEO Eq. (9), the factor k has been introduced:

$$k = 3F_{\text{osc}} \left(\frac{e^2}{m} \right) \quad (11)$$

The oscillator strength factor $F_{\text{osc}} = \gamma_r / (3\gamma_{\text{ceo}})$ is defined in the hypothesis that the atomic dipoles are fully aligned with the applied field. γ_{ceo} is the energy decay rate of the CEO model, e is the electron charge and m is the electron mass. Finally $\Delta N_{12} = N_1 - N_2$ is the electron population difference between the lower and upper energy levels involved in the transitions, N_1 and N_2 being the number of atoms per unit volume on two levels.

The polarization due to the host dielectric material in the frequency domain is defined as:

$$\mathbf{P}_{\text{host}}(\omega) = \varepsilon_0 \chi_{\text{host}} \mathbf{E}(\omega)$$

being χ_{host} the host material electric susceptibility. Therefore the frequency domain constitutive relation can be so expressed:

$$\mathbf{D}(\omega) = \varepsilon_{\text{host}} \mathbf{E}(\omega) + \mathbf{P}_{\text{at}}(\omega) \quad (12)$$

where $\varepsilon_{\text{host}}$ is the host dielectric constant given by $\varepsilon_{\text{host}} = \varepsilon_0 [1 + \chi_{\text{host}}]$.

By Fourier transforming the eq. (8), the susceptibility $\chi_{\text{at}}(\omega)$ for the resonant oscillator part in the laser medium can be obtained:

$$\chi_{\text{at}}(\omega) = \frac{\mathbf{P}_{\text{at}}(\omega)}{\varepsilon_{\text{host}} \mathbf{E}(\omega)} \quad (13)$$

Hence the resonant electric susceptibility is given by:

$$\chi_{\text{at}}(\omega) = \frac{3\gamma_r \lambda_a^3 \omega_a \Delta N}{4\pi^2} \frac{1}{\omega_a^2 - \omega^2 + j\omega \Delta\omega_a} \quad (14)$$

The $\chi_{\text{at}}(\omega)$ function is called complex Lorentzian lineshape.

It is worthwhile to outline that the excitation rate $\frac{\mathbf{e}(t) \cdot \mathbf{dp}(t)}{h\nu_s dt}$ in the Eq. (3,4), takes into account the emission and absorption properties of the active medium under examination. In fact while the material chromatic dispersion is linked to the real part of the resonant electric susceptibility $\chi_{\text{at}}(\omega)$, the gain coefficient α_m of the active medium is linked to the imaginary part of $\chi_{\text{at}}(\omega)$. Furthermore the gain coefficient α_m can be expressed in terms of the upward and downward cross sections.

Therefore, known the erbium experimentally measured absorption and emission cross sections of transitions $\sigma_{12}(\omega)$ and $\sigma_{21}(\omega)$, it is possible to evaluate the imaginary part χ'' of the resonant electric susceptibility $\chi_{\text{at}}(\omega)$ as:

$$\Delta_\sigma = N_1 \sigma_{12}(\omega) - N_2 \sigma_{21}(\omega) = \frac{2\pi}{\lambda_a} \chi''(\omega) \quad (15)$$

The Eq. (1-6, 8) have been implemented in a computer code based on the finite difference scheme; the excitation has been implemented by using the total-field/scatter-field scheme

while the first order Mur absorbing boundary conditions have been used to minimize the reflected wave contributions.

3. Numerical results

The structure investigated in this paper is a buried channel waveguide, depicted in Fig. 2, constituted by an Er-doped $\text{SiO}_2\text{-TiO}_2$ core with transversal dimensions equal to $1.8 \mu\text{m}$ surrounded by a substrate of SiO_2 . The length of the device is opportunely fixed in order to obtain a gain as high as possible. The refractive indices of the core and substrate media have been evaluated via the Sellmeier equation [11], in the whole wavelength range of the emission and absorption cross-sections by fitting the measured refractive indices reported in Table 1 [5]. Therefore, the core and the substrate refractive indices, at the operating wavelength $\lambda_s = 1532 \text{ nm}$, are equal to $n_{\text{core}} = 1.4650$ and $n_{\text{sub}} = 1.4452$, respectively.

Table 1. Optical properties of $\text{SiO}_2\text{-TiO}_2\text{:Er}$ waveguide

Substrate	SiO_2 glass
n_{sub} at 543.5 nm	1.4603 ± 0.0005
n_{sub} at 632.8 nm	1.4575 ± 0.0005
n_{sub} at 1550 nm	1.4450 ± 0.0005
Core	$\text{SiO}_2\text{-TiO}_2$
n_{core} at 543.5 nm	1.485 ± 0.002
n_{core} at 632.8 nm	1.482 ± 0.002
n_{core} at 1550 nm	1.462 ± 0.002
Film thickness b (μm)	1.8 ± 0.1

The analysis of the channel EDWA has been performed by exploiting the refractive effective index method [4]; the Maxwell equations have been reduced to a one-dimensional system, by reducing the single-mode channel waveguide to a bulk medium characterized by the refractive effective index $n_{\text{eff}} = 1.445937$ at the operating wavelength $\lambda_s = 1532 \text{ nm}$. Moreover, the experimentally measured erbium emission and absorption cross sections [4] shown in Fig. 3, which are linked to the imaginary part of the $\chi_{\text{at}}(\omega)$ (eq.17), have been used to evaluate the difference $\Delta_{\sigma} = N_1\sigma_{12}(\omega) - N_2\sigma_{21}(\omega)$.

To be included in the time domain code, the quantity Δ_{σ} has been fitted by means of five Lorentzian lineshape curves, the significant parameters of which are reported in Table 2. Figure 4 shows the Δ_{σ} curve derived by the measured values and the perfectly reconstructed curve.

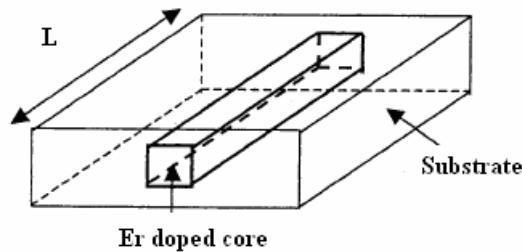


Fig. 2. Buried channel waveguide

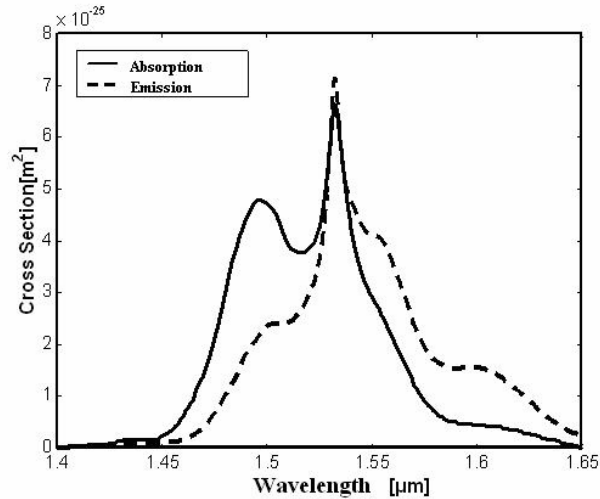


Fig. 3. Experimentally measured erbium emission and absorption cross sections

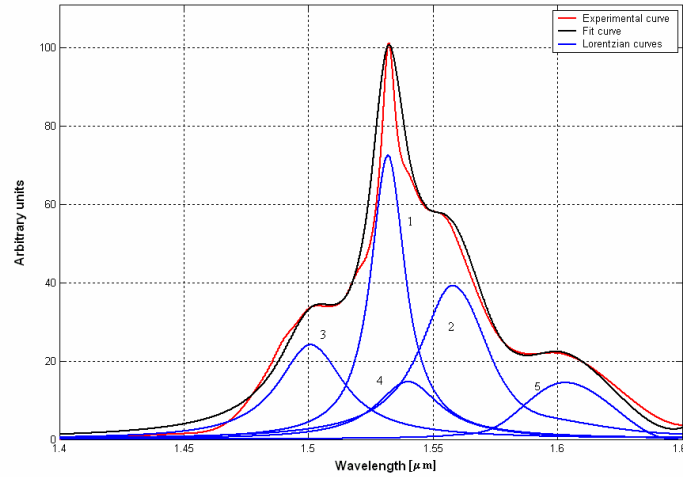


Fig. 4. Measure derived $\Delta\sigma$ curve and reconstructed $\Delta\sigma$ profile. Five Lorentzian lineshape are also shown.

Table 2. Fundamental parameters of the Lorentzian functions used in the fitting procedure.

Lorentzian functions	$\Delta\omega_a$ [Hz]	λ_a [μm]
1	1.3333×10^{13}	1.532
2	2.5000×10^{13}	1.558
3	2.7027×10^{13}	1.501
4	2.5000×10^{13}	1.540
5	1.3333×10^{13}	1.600

To validate the code, we have investigated the erbium doped structure by considering as excitation source a sine function at the operating λ_s wavelength and the obtained results have been compared with those evaluated in the frequency domain [5]. The simulation data are summarized in Table 3. An excellent agreement between the results has been obtained: as an example, for a device length equal to $L = 1$ mm, the time domain transmission coefficient T_t is equal to 1.0498 while the frequency domain transmission coefficient T_f is 1.0494. The same accuracy has been obtained when the concentration quenching effects have been neglected, i.e. the erbium energy system is reduced to a three-level system. As expected, the transmission

coefficient improvement verifies when the concentration quenching phenomena are neglected. In fact in this case, for the same device length, we have obtained $T_t = 1.0654$ and $T_f = 1.0653$, respectively.

Table 3. Simulation input data

Pump signal power P_p	300 mW
Input signal power P_s	1 μ W
Loss coefficient	0.4 dB/cm
Pump signal wavelength λ_p	980 nm
Input signal wavelength λ_s	1532 nm
Erbium concentration	$2.2 \cdot 10^{26}$ ions/m ³
Effective refractive index	1.445937
Longitudinal step Δz	$15.32 \cdot 10^{-9}$ m
Time step Δt	$3 \cdot 10^{-17}$ s
Cross Section (at the wavelength λ_p) σ_p	$2.5 \cdot 10^{-25}$ m ²
$C_{up} = C_3$	$5 \cdot 10^{-23}$ m ³ /s
C_{14}	$3.5 \cdot 10^{-23}$ m ³ /s
Radiative relaxation rate γ_r	140.85 s ⁻¹
$\tau_{43} = \tau_{32}$	$1 \cdot 10^{-9}$ s
τ_{21}	$7.1 \cdot 10^{-3}$ s

Figure 5 shows the evaluated time evolution of population densities on the four different levels of the erbium system, by assuming a time step equal to $t = 3 \cdot 10^{-12}$ s. After the pump signal application, the metastable energy level 2 becomes populated to the prejudice of the ground level 1. The energy levels 3 and 4 do not reach significant population densities because of their unstable nature. To consider the population inversion effectively verified, the quantity Δ_σ must be positive and the population density N_2 must be equal to 95% of the starting population density N_1 . In the case under examination, only $t = 30 \mu$ s are sufficient to obtain the population inversion.

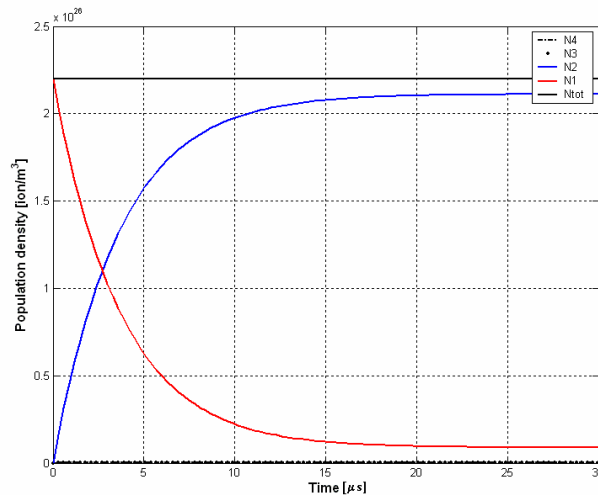


Fig. 5. Temporal evolution of the population densities of the erbium system

Figure 6 shows the transmission coefficient obtained simulating a structure 5 mm long excited by an input signal having the following shape:

$$e(t) = \sin(\omega_s(t - t_0)) \exp\left(-\left((t - t_0)/v\right)^2\right)$$

where t_0 is the time at which the pulse is centered and v is the pulse FWHM.

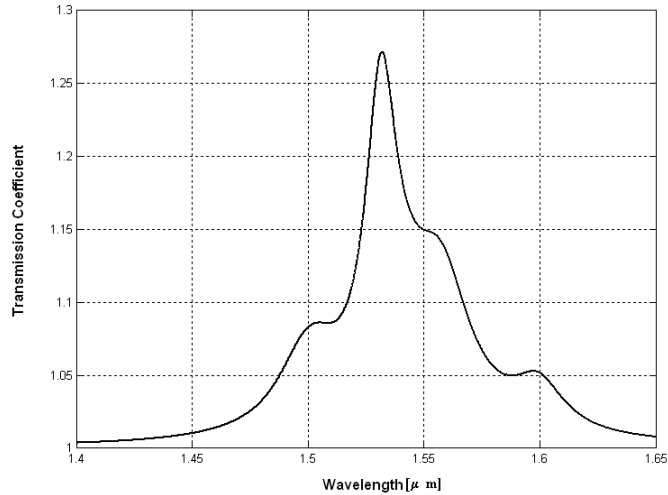


Fig. 6. Transmission spectrum of an active waveguide 5 mm long

The transmission coefficient shape follows the emission and absorption cross section frequency lineshape. It reaches the value of $T = 1.27$ at the signal wavelength and increases by further increasing the device length. The transmission coefficient as a function of the pump signal power, for a constant input signal power $P_s = 1 \mu\text{W}$, has been reported in Fig. 7 for three different values of the device length $L = 1 \text{ mm}$, $L = 2.5 \text{ mm}$ and $L = 5 \text{ mm}$; it increases by increasing the pump signal power because of the increasing of the meta-stable energetic level population. For a pump signal power value of about $P_p = 100 \text{ mW}$, the transmission coefficient becomes almost constant showing a saturation-like behaviour.

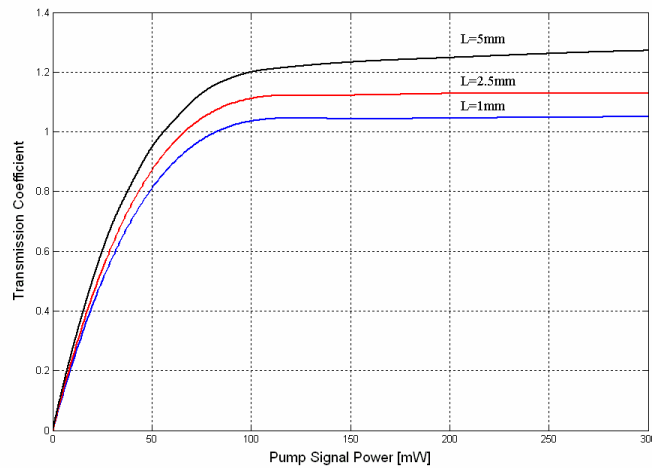


Fig. 7. EDWA transmission coefficient as a function of pump signal power P_p for an input signal power of $1 \mu\text{W}$.

Figure 8 shows the transmission coefficient of the same waveguide, as a function of erbium ion concentration. The simulations have been performed by considering a pump signal power $P_p = 300$ mW and an input signal power $P_s = 1$ μ W for the three device lengths. The transmission coefficient increases by increasing the erbium ion concentration; the effects of concentration quenching are not evident due to the considered short device lengths.

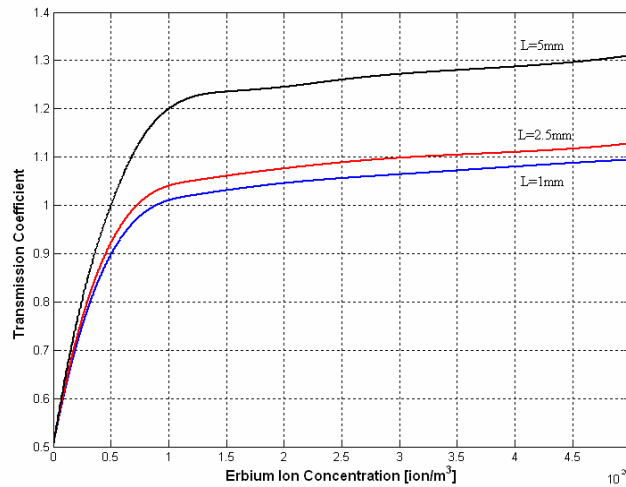


Fig. 8. EDWA transmission coefficient as a function of erbium ion concentration

4. Conclusion

In this paper the time domain analysis of the amplification phenomena in erbium doped silica-titania waveguide is reported. The simulation model, based on the ADE-FDTD method combined with the erbium rate equations, takes into account the simultaneously input and pump signal propagation, the secondary transitions pertaining to the ion-ion interactions and exploits the optical, spectroscopic and geometrical parameters measured on the fabricated waveguide.

Acknowledgments

This work was partially sponsored by the research contract FIRB 2001, "Modelling and numerical methods of photonic devices for high capacity optical networks".